Pharm Res (2014) 31:660–669
DOI 10.1007/s11095-013-1188-z

RESEARCH PAPER

Antiangiogenic Effect of Docetaxel and Everolimus as Individual and Dual-Drug-Loaded Micellar Nanocarriers

Gyan P. Mishra • Bhuvana Shyam Doddapaneni • Duc Nguyen • Adam W. G. Alani

Received: 19 May 2013 / Accepted: 9 August 2013 / Published online: 25 September 2013

ABSTRACT

Purpose The *in vitro* inhibitory effect of Docetaxel (DTX) and Everolimus (EVR) alone and together in poly(ethylene glycol)-*block*-poly(D,L-lactic acid) (PEG-*b*-PLA) nanocarriers on angiogenic processes and acute toxicity in mice was evaluated.

Methods PEG-*b*-PLA DTX and/or EVR nanocarriers were characterized for size, drug loading, stability, and drug release. Cell proliferation, tubule formation, and migration studies were performed in Human Umbilical Vein Endothelial Cells (HUVEC) and Maximum Tolerated Doses (MTD) studies were in mice.

Results DTX and EVR loading was 1.93 and 2.00 mg/mL respectively with similar solubilities for dual-drug micelles. All micelles were below 30 nm with diffusion controlled drug release. The IC_{50} for DTX, EVR micelles were, 6.80 ± 0.67, 18.57 ± 2.86 and 0.65 ± 0.11 nM respectively with a synergistic inhibitory effect for dual-drug nanocarriers. Significant inhibition of tube formation occurred upon treatment with dual-drug nanocarriers as compared to individual micelles. EVR presence in dual-drug nanocarriers was able to significantly increase the inhibition of the migration of HUVEC by DTX. The MTDs for EVR, DTX and dual-drug micelles were 50, 30 and 20 mg/kg for each respectively.

Conclusions DTX-EVR dual-drug nanocarriers have antiangiogenic effects *in vitro* mediated through cellular angiogenic process and possess clinically relevant MTD.

KEY WORDS antiangiogenesis · combination therapy · polymeric micelles

G. P. Mishra • B. S. Doddapaneni • D. Nguyen • A. W. G. Alani
Department of Pharmaceutical Sciences, College of Pharmacy
Oregon State University, Corvallis, Oregon, USA

A. W. G. Alani (✉)
Division of Pharmaceutical Sciences, College of Pharmacy
Oregon State University, Corvallis, Oregon 97331, USA
e-mail: Adam.Alani@oregonstate.edu

INTRODUCTION

Angiogenesis is the process of forming new blood vessels from a pre-existing vascular bed (1). In angiogenesis-dependent diseases the body losses control over angiogenesis resulting in excessive or insufficient growth of new blood vessels (2–4). Excessive angiogenesis occurs in diseases such as cancer, diabetic blindness, age-related macular degeneration, rheumatoid arthritis, psoriasis and more than 70 other conditions (4). In these conditions, new blood vessels feed diseased tissue, destroy normal tissue and in the case of cancer, angiogenesis allows tumor metastases. Excessive angiogenesis occurs when diseased cells produce an abnormal amount of angiogenic growth factors such as VEGF, PDGF, FGF and EGF resulting in minimizing the effect of endogenous angiogenesis inhibitors such as angiostatin, endostatin, thrombospondin-1, to name a few (3). Antiangiogenic therapies are used to treat these conditions by inhibiting or slowing down new blood vessel formation and growth. Currently the Food and Drug Administration has approved thirteen drugs in the United States for cancer treatment with significant antiangiogenic activities. These drugs affect tumor angiogenesis by interfering with cell signaling pathways that are essential for angiogenic and proliferation processes. The use of antiangiogenic drugs for cancer treatment was heralded as a new treatment modality due to the lower anticipated tumor-acquired resistance over time (5). Unfortunately, clinical experience has demonstrated that acquired resistance to antiangiogenic therapeutic strategies is possible since many patients whose tumors initially respond to drugs such as bevacizumab, sorafenib, or sunitinib become nonresponsive, often within months of therapy initiation (6). The resistance to antiangiogenic drugs in cancer patients has triggered the need to establish a new treatment scheme that can actively target angiogenesis in the cancer without acquiring resistance.

One approach to overcome this resistance is the implementation of co-targeting strategies, where multiple mechanisms

of drug action can target neovascular angiogenic endothelial cells within the cancer tissue. Some of the chemotherapeutic drugs such as taxanes and mammalian target of rapamycin (mTOR) inhibitors have both cytotoxic and secondary antiangiogenic effects in tumor tissues. However, their antiangiogenic capacities are not fully manifested, due in large part to limitations in dosing regimens and available drug formulations (7–10). Docetaxel (DTX) and Everolimus (EVR) a microtubule-stabilizing agent and an allosteric mTOR inhibitor respectively, are chemotherapeutic agents that have been approved in the U.S. for the treatment of multiple cancers. Both compounds individually have shown strong antiangiogenic effect in *in vitro* and *in vivo* models as well as in the clinical setting. However, the combined antiangiogenic response of DTX and EVR has neither been examined *in vitro* nor *in vivo* models.

Taxanes including DTX are among the most potent antiangiogenic chemotherapeutic agents, this effect is manifested in the human endothelial cells which are extremely sensitive to these compounds at ultra-low concentrations that have no effect on other cell types such as tumor cells, fibroblasts, epithelial cells or smooth muscle cells (11–13). At these non-cytotoxic concentrations DTX appeared to inhibit VEGF induced endothelial cell migration by the reduction of the cytoplasmic chaperone *Heat-Shock protein 90* through the induction of its proteasomal degradation (14). EVR has shown antiangiogenic effect in *in vitro* and *in vivo* nonclinical models (15,16). At the molecular levels EVR can block angiogenesis by inhibiting of hypoxia-inducible transcription in factors-1-alfa (H1Fα) translation as well as by intercepting vascular endothelial growth factor (VEGF/VEGFR) and or platelet-derived growth factor (PDGF/PDGFR) signaling cascade (17).

Polymeric micelles are colloidal particles with a size usually within the range of 15–150 nm (18). Over the last 20 years polymeric micelles have emerged as viable drug delivery system for poorly water-soluble drugs especially for cancer therapy (18,19). Currently there are five polymeric micellar formulations for cancer therapy under clinical trials (19). Recently new drug delivery systems based on PEG-*b*-PLA polymeric micelles have been developed for the concurrent delivery of multiple anticancer drugs. These multi-drug loaded micelles have shown a synergistic inhibition of different cancers models *in vitro* and *in vivo* (20–22). Both DTX and EVR are poorly water-soluble compounds with intrinsic water solubilities at 1.9 and 9.6 μg/mL respectively (23,24). PEG-*b*-PLA micelles can provide a unique platform as a nanocarrier for DTX (20,25) and EVR individually and in combination. These nanocarriers can solubilize DTX and EVR and act as a delivery system for these drugs individually and in combination for the treatment of excessive angiogenesis in cancer and other diseases.

The goal of this work is to formulate PEG-*b*-PLA micellar nanocarriers for the delivery of DTX and EVR individually and in combination and evaluate their antiangiogenic activity *in vitro* on three cellular processes that are essential for angiogenesis, which include proliferation, tube formation and migration (26,27). In addition, we aim to evaluate the acute toxicity of these nanocarriers *in vivo*. We *hypothesize* that DTX and EVR individual micellar nanocarriers will exert antiangiogenic effect and a synergistic effect for the dual-drug loaded nanocarriers. In addition, all micellar nanocarriers will show no acute toxicity *in vivo* at therapeutically relevant concentrations.

MATERIALS AND METHODS

Materials

DTX and EVR were purchased from LC Laboratories (Woburn, MA). HUVEC cells and endothelial growth medium 2 were purchased from PromoCell (Heidelberg, *Germany*). Cells were cultured as per the manufacturer instructions and all experiments were performed between passages 2 and 6. Diblock copolymers PEG_{2000}-*b*-PLA_{1800} (Mn = 3800, Mw = 4100 and PI = 1.1) and PEG_{4000}-*b*-PLA_{2200} (Mn = 6100, Mw = 6500 and PI = 1.06) were purchased from Advanced Polymer Materials Inc. (Montreal, CAN). CellTiter-Blue® Cell Viability Assay kit was obtained from Promega Inc. (Madison, WI). All other reagents of analytical grade were purchased from VWR International, LLC (Radnor, PA) and Fisher Scientific Inc. (Fairlawn, NJ).

Preparation of Drug Loaded Micelles

DTX, EVR and DTX-EVR dual-drug loaded PEG-*b*-PLA micelles (DDM) were prepared by solvent casting method as reported previously (20,21,25,28). Briefly, for the preparation of DTX or EVR individual micelles, 15 mg polymer (PEG_{2000}-*b*-PLA_{1800}) and 2 mg of DTX or EVR was dissolved in 0.5 ml of acetonitrile, which was evaporated under reduced pressure to form a thin polymeric film. Micelles were obtained by rehydration of polymeric film with 0.5 ml deionized water and then micellar solution was filtered using a 0.45 μm filter. For the DDM, DTX (2 mg), EVR (2 mg), and PEG_{2000}-*b*-PLA_{1800} (15 mg) polymer were dissolved in 0.5 ml acetonitrile and the micelles were prepared as mentioned above. A second set of DTX or EVR or DDM were prepared using PEG_{4000}-*b*-PLA_{2200} polymer using the same procedure.

Reverse Phase High Performance Liquid Chromatography (RP-HPLC) Analysis for Drug Loading

The drug loading was determined using Shimadzu HPLC system consisting of LC-20 AT pump and SPD M20 a diode array detector. The analysis was performed using Zorbax C8 Column (4.6 × 75 mm, 3.5 μm) in isocratic mode with

acetonitrile/water (62/38) containing 0.1% phosphoric acid and 1% methanol at a flow rate of 1 ml/min and injection volume of 10 µL. Column temperature was kept at 40°C. The DTX and EVR peaks were monitored at 227 and 279 nm respectively. The retention times for DTX and EVR were 1.7 and 5.7 min respectively. All measurements were performed in triplicate and loading data is presented as Mean ± SD.

Particle Size Analysis

Particle size of polymeric micelles was measured by dynamic light scattering (DLS) using a Malvern Nano ZS (Malvern Instruments Inc., U.K.). Samples were diluted 20 times with deionized water to yield final polymer concentration of 1.5 mg/ml. The intensity of He-Ne laser (633 nm) was measured at 173°. All measurements were performed at 25°C after pre-equilibration for 2 min. The particle size was measured in triplicates and Z-average size was reported as the Mean ± SD and polydispersity index (PDI).

In Vitro Drug Release Study from Individual Micelles and Dual-Drug-Loaded Micelles

DTX and EVR individual and DDM were prepared as described above ("Preparation of Drug-Loaded Micelles" section), and a sample of 2.5 mL was loaded into a Slide-A-Lyzer® (Thermo Scientific Inc.) dialysis 3.0 mL cassette with a MWCO of 7,000 g/mol. This MWCO was chosen to enable the free drug(s) along with the unassociated polymer molecules to diffuse freely out of the cassette and thereby ensure sink conditions. Four cassettes were used in each experiment ($n = 4$). The cassettes were placed in 2.5 L of 10 mM phosphate buffer at pH 7.4, which was changed every 3 h to ensure sink conditions and the temperature was maintained at 37°C. The sampling time intervals were 0, 0.5, 1, 2, 3, 6, 9, 12, 24, and 48 h. A sample of 150 µL at each time point was withdrawn, and the cassette was replenished with fresh 150 µL of buffer. Samples were analyzed by RP-HPLC for drug content. To evaluate drug release kinetics in more detail, the drug release data were curve-fitted assuming that the drug(s) were released by simple diffusion using a one phase exponential association equation. The time needed to reach 50% of drug release, $t_{1/2}$ of each drug in individual or DDM and the goodness of fit were calculated. The curve fitting analysis was performed with GraphPad Prism version 5.04 for Windows, GraphPad Software, San Diego California USA, www.graphpad.com.

HUVEC Cell Proliferation Assay

HUVEC cells were seeded at the density of 5,000 cells/well in 96 well plates and allowed to attach for 48 h at 37°C. After incubation, cells were treated with individual or DDM. DTX concentration range was 0.02–20 nM while EVR concentration range was 20–2000 nM in individual micelle treatments. While for the DDM; DTX:EVR (1:1) molar ratio the concentration range for each drug was from 0.02 to 20 nM. Cell viability was determined after 48 h by treatment with 20 µL of CellTiter-Blue® reagent followed by one hour of incubation at 37°C and fluorescence ($560_{Ex}/590_{Em}$) signal was measured, all measurements were performed in quadruplicate. The drug concentration at 50% growth inhibition (IC_{50}) was determined by the *linearized median-effect plot* using Compusyn software (Version 1.0, ComboSyn Inc., U.S.) (29). This software is based on Chou and Talay median-effect method in which the median-effect equation is a general equation for dose-effect relationship derived from the mass-action law principle that takes into account the potency and the shape of dose-effect curve. The dose-effect relationship as shown by the mass action law is mathematically described below:

$$\frac{f_a}{f_u} = \left(\frac{D}{D_m}\right)^m$$

Where; f_a and f_u represent the effect while D is the dose causing the effect. The dose effect curve can be linearized by the *median effect plot* where $x = log(D)$ and $y = log(f_a/f_u)$

$$log\left(\frac{f_a}{f_u}\right) = mlog(D) - mlog(D_m)$$

where f_a is the fraction of cells affected upon drug treatment, f_u is the fraction of cells unaffected upon drug treatment, $f_u = (1 - f_a)$, D is the dose of the drug, D_m is the dose that is required to produce a median effect (e.g., IC_{50}, ED_{50}, or LD_{50}), and m is the slope of the line.

Combination Index (CI) Analysis

The combination effect of DTX and EVR loaded in DDM on HUVEC cells proliferation (see "HUVEC Cell Proliferation Assay" section) was evaluated with Compusyn software using the Combination index (CI) analysis (29,30). CI value obtained from the software represents the effect of combination. CI value of 1 indicates additive effect, CI>1 indicates antagonism and CI<1 indicates synergism. CI value of DTX and EVR were computed using the following formula:

$$CI = \frac{(D)_1}{(Dx)_1} + \frac{(D)_2}{(Dx)_2}$$

where is $(D_x)_1$ and $(D_x)_2$ are the inhibitory concentration of drug 1 and drug 2 alone respectively. $(D)_1$ and $(D)_2$ are the drug 1 and 2 concentration respectively. The data was

represented as F_a-CI Plot (Chou-Talalay Plot) a plot of CI on y- axis as a function of effect level (F_a) on the x- axis.

In Vitro Endothelial Tube Formation Assay

Matrigel was thawed overnight at 4°C in the ice bath and then 50 µL of solution was used to coat 96 well plates. The plates were then incubated at 37°C for 60 min to ensure complete gelation of the matrix. HUVEC cells were then seeded into 96 well plates at a cell density of 20,000 cells/well and allowed to incubate for 18 h at 37°C. The total tube length and area were quantified using NIH ImageJ analysis software (31). Cells were treated with different concentrations of DTX (0.01, 0.1 and 1 nM), EVR (10, 100 and 1000 nM) individual micelles and DDM.

Migration Assay

HUVEC cell migration process was analyzed using xCELLigence RTCA DP instruments (Roche Applied Sciences, Germany). The system measures the electrical impedance which indicates the number of cells that migrated from the apical to the basolateral chamber in response to a chemoattractant. A change in electrical impedance was recorded in terms of *cell index* number. CIM-Plates 16 were coated with 20 µg/ml of fibronectin for 1 h. HUVEC cells were starved for 4 h with serum free medium and seeded on pre-coated fibronectin plates at a density of 15,000 cells/well. A change in electrical impedance was monitored every 10 min for 48 h. In the basolateral chamber, HUVEC cells complete medium was used as control and DTX, EVR and DDM in complete medium as treatment groups were added in quadruplicates. The compiled data was presented as Mean±SD. Significant differences between treatment group means was evaluated using one way ANOVA with Bartlett's test for equal variances and Bonferroni's multiple comparison test, using a threshold value (α) of 0.05.

Acute Toxicity Study

The acute toxicity of DTX, EVR individual and DDM was evaluated in 6 to 8-week-old FVB albino female mice (The Jackson Laboratory (Bar Harbor, ME) and housed in ventilated cages with free access to water and food. DTX, EVR or DDM were prepared freshly and reconstituted with saline and sterilized with 0.22 µm filter prior to injection. Six groups of mice ($n=24$; 4/group) were injected, i.v. (tail vein) with saline, DTX individual micelles, EVR individual micelle or DTX:EVR (1:1) DDM. The total number of injections for the treatment protocol was three and the injections were performed on days 0, 4 and 8 with the volume of injection between 80 and 180 µL. DTX individual micelles were injected at 40 or 30 mg/kg, EVR individual micelles were injected at 60 or 50 mg/kg and DDM were injected at total concentration of both drugs at 60 or 40 mg/kg (30 or 20 mg/kg for each drug).

Acute toxicity (dose limiting toxicity, DLT) was defined as the dose that causes a median body weight loss of ≥15% *versus* negative control (saline) and causes either remarkable change in general appearance or death. Mice with a weight loss ≥15% were euthanized because changes of this magnitude often indicate lethal toxicity. The maximum tolerated dose (MTD) was defined as dose level just below the DLT for a given formulation. Compiled data was presented as Mean±SD. The animal work was conducted in compliance with NIH guideline and Institutional Animal Care and Use Committee policy in Oregon State University for End-Stage Illness and Pre-emptive Euthanasia based on Humane Endpoints Guidelines.

RESULTS

Drug Loading and Retention in Micelles

Individual and dual-drug PEG-*b*-PLA micelles were formulated for DTX, EVR and their combination (Fig. 1). PEG_{4000}-*b*-PLA_{2200} micelles loaded with DTX were able to solubilize 1.74±0.1 mg/mL , while EVR loaded micelles were able to solubilize 2.00±0.09 mg/mL (Fig. 2). The DTX-EVR dual-drug PEG_{4000}-*b*-PLA_{2200} micelles were able to load DTX and EVR at 1.91±0.1 mg/mL at 2.0±0.10 mg/ml respectively (Fig. 2).

PEG_{2000}-*b*-PLA_{1800} micelles increased the water solubility of DTX to 1.93±0.1 mg/mL (Fig. 2). Initial loading of PEG_{2000}-*b*-PLA_{1800} with EVR or DDM were similar to PEG_{4000}-*b*-PLA_{2200} but these micelles were not stable post 5 h at 25°C as demonstrated by drug(s) precipitation.

DTX in PEG_{2000}-*b*-PLA_{1800} and EVR in PEG_{4000}-*b*-PLA_{2200} individual micelles demonstrated excellent stability for more than 24 h at 25°C with more than 98% drug was retained in solution. Drug retention studies also indicated that the PEG_{4000}-*b*-PLA_{2200} DTX micelles were not stable due to drug precipitation. PEG_{4000}-*b*-PLA_{2200} DDM demonstrated

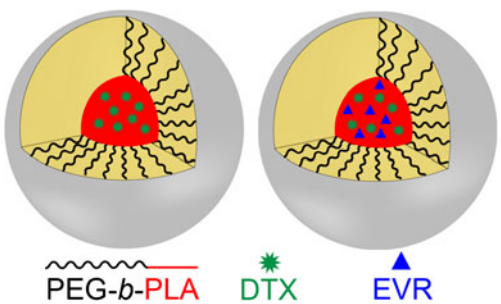

Fig. 1 Schematic representation of individual and DDM.

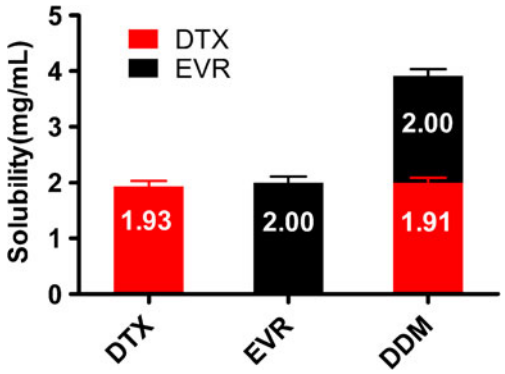

Fig. 2 Aqueous solubility of DTX in PEG_{2000}-*b*-PLA_{1800} individual micelles, EVR in PEG_{4000}-*b*-PLA_{2200} individual micelles and DTX-EVR DDM in PEG_{4000}-*b*-PLA_{2200} micelles (Mean ± SD, $n = 4$).

higher drug stability at 25°C for more than 24 h in comparison to PEG_{2000}-*b*-PLA_{1800} DDM. Therefore, all subsequent experiments were performed using PEG_{4000}-*b*-PLA_{2200} for EVR or DDM and PEG_{2000}-*b*-PLA_{1800} DTX micelles.

Particle Size Analysis

PEG_{2000}-*b*-PLA_{1800} DTX micelle sizes were 18.05±0.06 nm (PDI=0.079±0.013), while PEG_{4000}-*b*-PLA_{2200} EVR and DDM had sizes of 33.80±0.05 nm (PDI=0.113±0.010) and 34.09±0.24 nm (PDI=0.137±0.004) respectively (Fig. 3). All prepared micelles showed unimodal distribution with a PDI value of less than 0.2.

In Vitro Drug Release Study from Individual Micelles and DDM

The release profile of DTX and EVR from individual and DDM were evaluated in pH 7.4 buffer at 37°C over 48 h by a simple dialysis method. DTX release profile from PEG_{2000}-*b*-PLA_{1800} individual micelles and PEG_{4000}-*b*-PLA_{2200} DDM is depicted in (Fig. 4a) with about 90% DTX released from both micelles over 48 h. EVR release profile from PEG_{4000}-*b*-PLA_{2200} individual and DDM is illustrated in (Fig. 4b). The release of EVR from individual micelle after 48 h was 60.0± 2.4% while the EVR release from DDM after 48 h was 49.2± 0.9%. The time needed to reach 50% of drug release ($t_{1/2}$) of each drug in individual or DDM and the goodness of curve-fitting (r^2) were calculated. The $t_{1/2}$ for DTX in individual and DDM were 10.00 and 8.86 h respectively with r^2 values of 0.986 for the individual micelle and 0.987 for the DDM (Fig. 4a). The $t_{1/2}$ of EVR in individual micelles was 35 h however with an r^2 value of 0.820 indicating a poor fit to the assumed model (Fig. 4b). On the other hand the $t_{1/2}$ for EVR in DDM was approximately 48 h with an r^2 value of 0.955 which is a good fit to the assumed model (Fig. 4b). The goodness of curve-fitting (r^2) for all micelles except EVR individual micelles, were above 0.950 which means that the assumption for 1st order release was a good approximation to explain drug release from individual micelles and DDM.

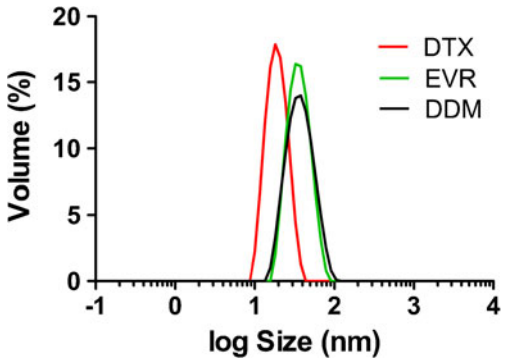

Fig. 3 Particle size distributions (volume-weighted) for DTX in PEG_{2000}-*b*-PLA_{1800} individual micelles, EVR in PEG_{4000}-*b*-PLA_{2200} individual micelles and DTX-EVR DDM in PEG_{4000}-*b*-PLA_{2200} micelles.

HUVEC Cell Proliferation Assay

The antiproliferative effect of DTX, EVR individual and DDM were evaluated in HUVEC cells. The cytotoxicity of individual and DDM (1:1) micelles demonstrated a dose dependent decrease in cell viability. For all micelles the drug concentration at 50% growth inhibition (IC_{50}) was determined by the *linearized median-effect plot* (Fig. 5). The IC_{50} values of DTX and EVR in individual micelles were 6.80±0.67 nM and 18.57

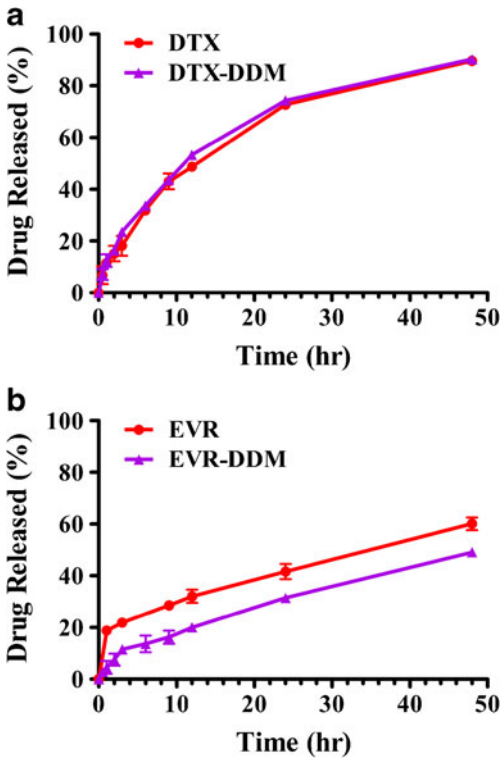

Fig. 4 *In vitro* drug release profiles of (**a**) DTX loaded in individual micelles and DDM (**b**) EVR loaded in individual micelles and DDM. (Mean ± SD, $n = 4$).

±2.86 nM respectively (Fig. 6). The combination of DTX and EVR in DDM demonstrated strong dose dependent inhibition with IC_{50} value at 0.65±0.11 nM (Figs. 5 and 6).

Combination Index (CI) Analysis

To further analyze whether DTX and EVR combination are synergistic, additive or antagonistic, against HUVEC proliferation, the CI values for the various dosing ratios were calculated using Compusyn software. The calculated CI values of DTX and EVR in DDM at different concentrations were well below 1.0 (Fig. 7) indicating significant synergistic antiproliferative effect against the HUVEC across different concentrations of the DTX and EVR combination.

In Vitro Endothelial Tube Formation Assay

HUVEC were treated and cell differentiation was monitored *in vitro* by tube formation on matrigel matrix. HUVEC cells without treatment resulted in formation of regular capillary like tubular structures (Fig. 8a). DTX loaded PEG_{2000}-*b*-PLA_{1800} micelles at 1 nM reduced tube formation area by 40.14±10.25% (Fig. 8b) while DTX micelles at 0.1 and 0.01 nM showed no significant reduction in the tube formation area compared to control. EVR loaded PEG_{4000}-*b*-PLA_{2200} micelles at 1,000 nM showed reduction in tube formation areas by 53.87±14.80% (Fig. 8c) while EVR micelles at 100 and 10 nM showed no significant reduction in the tube formation area compared to control. The DTX and EVR in DDM demonstrated significant reduction in tube formation process in comparison to DTX or EVR individual micelles. DTX and EVR combination in DDM at 0.5 nM and 500 nM respectively showed reduction in the tube formation area by 67.25±7.60% (Fig. 8d).

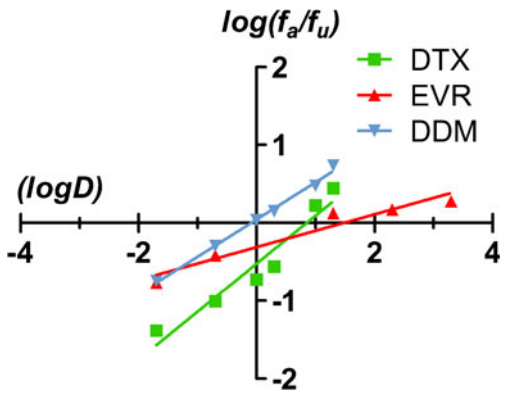

Fig. 5 Linearized median-effect plot to calculate the IC_{50} (*Dm*) for DTX, EVR individual micelles and DDM. Linear regression was applied to the experimental data in order to obtain the value for *Dm*, and *m* parameters. The squared correlation coefficient r^2 is a measure of the overall precision of the linear regression, r^2 for DTX, EVR, DDM are 0.931, 0.939 and 0.993 respectively.

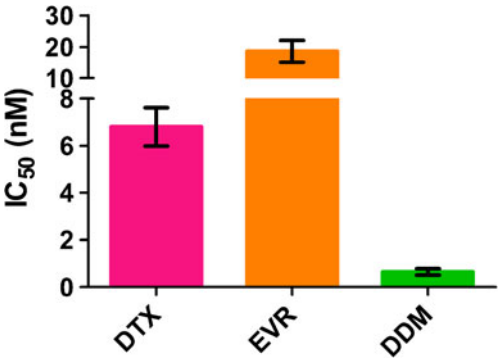

Fig. 6 IC_{50} values of DTX and EVR as individual micelles or DDM in HUVEC (Mean ± SD, $n = 4$).

Migration Assay

To assess the effect of drug loaded polymeric micelles on endothelial cell migration; real time migration using xCELLigence RTCA DP Instrument was used. The cell index value indicates the number of cells that migrate in response to a chemoattractant. By plotting the *cell index* values over *time*, a signature real-time cellular migration (RTCM) profile can be generated to monitor HUVEC migration in real time. We observed dose-dependent significant inhibition of HUVEC migration with DTX loaded PEG_{2000}-*b*-PLA_{1800} micelles at different concentration below 1 nM and the lowest concentration of DTX significant inhibition in migration was 0.005 nM (Fig. 9). In contrast, EVR PEG_{4000}-*b*-PLA_{2200} micelles did not show any significant inhibitory effect at 0.005 nM (Fig. 9). However, the EVR individual micelles showed strong inhibitory effect on migration on HUVEC at different concentrations above 0.005 nM (data not shown). Interestingly, in case of DTX:EVR (1:1) DDM at 0.005 nM each (total of 0.01 nM) showed significant inhibition in cell migration compared to control and DTX individual micelle at 0.005 nM (Fig. 9). These findings confirm the synergistic/additive effect of DDM on HUVEC cell migration process.

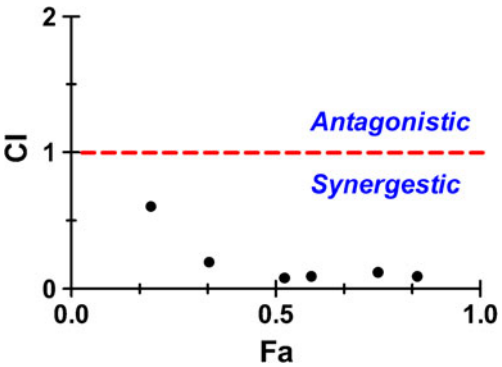

Fig. 7 *Fa-CI* plots of DTX and EVR combination in HUVEC cells. Cells were treated with DTX-EVR DDM at different concentrations.

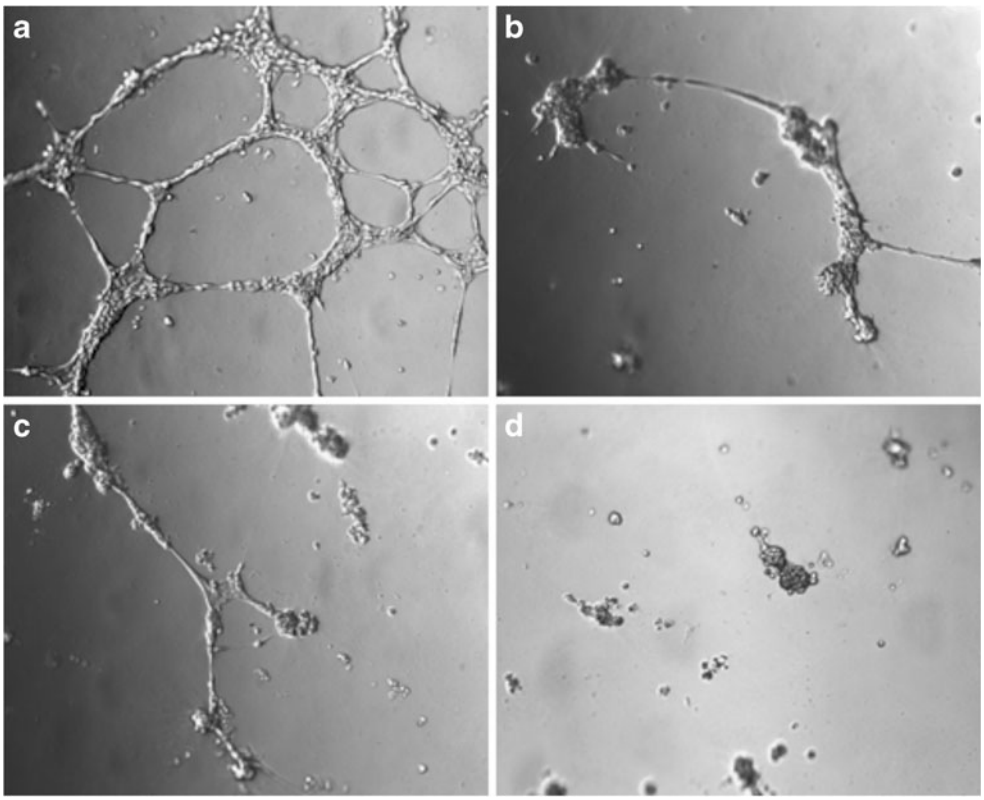

Fig. 8 Tube formation assay (**a**) control, (**b**) DTX micelles (1 nM), (**c**) EVR micelles (1,000 nM), (**d**) co-administration of DTX (0.5 nM) and EVR (500 nM) micelles.

Acute Toxicity Study

Mice were injected with EVR individual micelles at 60 and 50 mg/kg ($n=8$; 4/group). Mice injected with the 60 mg/kg EVR showed acute toxicity represented by lower extremity paralysis after the second injection (day 7). The second group of mice injected i.v., three times on day 0, 4, and 8 with EVR micelle at 50 mg/kg showed no sign of acute toxicity (Fig. 10a). DTX individual micelles were injected i.v., three times on day 0, 4, and 8 into 2 groups of mice (total $n=8$; 4/group) at 40 and 30 mg/kg. The first group injected with 40 mg/kg DTX showed acute toxicity after the third injection (day 16) represented by lost in weight > 15%. The second group injected with 30 mg/kg showed no sign of acute toxicity (Fig. 10b). DDM loaded with DTX:EVR (1:1) were injected i.v., three times on day 0, 4, and 8 into 2 groups of mice (total $n=8$; 4/group) at 30 mg/kg (for each drug, total of 60 mg/kg) and 20 mg/kg (for each drug, total of 40 mg/kg) . The first group injected with 30 mg/kg showed acute toxicity after the third injection (day 13) represented by lower extremity paralysis. The second group injected with 20 mg/kg showed no signs of acute toxicity (Fig. 10c). Treatment groups for individual and DDM showed no toxicity upon monitoring for an additional 39 days and all animal showed no signs of acute toxicity (data not shown) during this time. Thus, the MTD doses for the EVR, DTX and DDM were 50 mg/kg, 30 mg/kg and 20 mg/kg for each individual drug for a total of 40 mg/kg. For all the animals that showed acute toxicity, the experiments were stopped immediately and the animals were humanly euthanized in compliance with the guideline stated above.

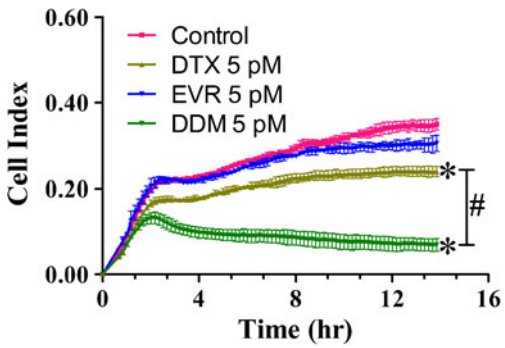

Fig. 9 Real-time cellular migration profile (RTCM) for HUVEC cells treated with: DTX individual micelles (0.005 nM), EVR individual micelles (0.005 nM), and DDM with DTX 0.005 nM and EVR 0.005 nM. * Represents significant difference from untreated control and # represents significant difference between DTX individual micelle and DDM. (Mean ± SD, $n=4$).

DISCUSSION

The main aim of our work is to develop a new treatment modality to overcome the acquired resistance to antiangiogenic therapy. This resistance can be potentially overcome by the

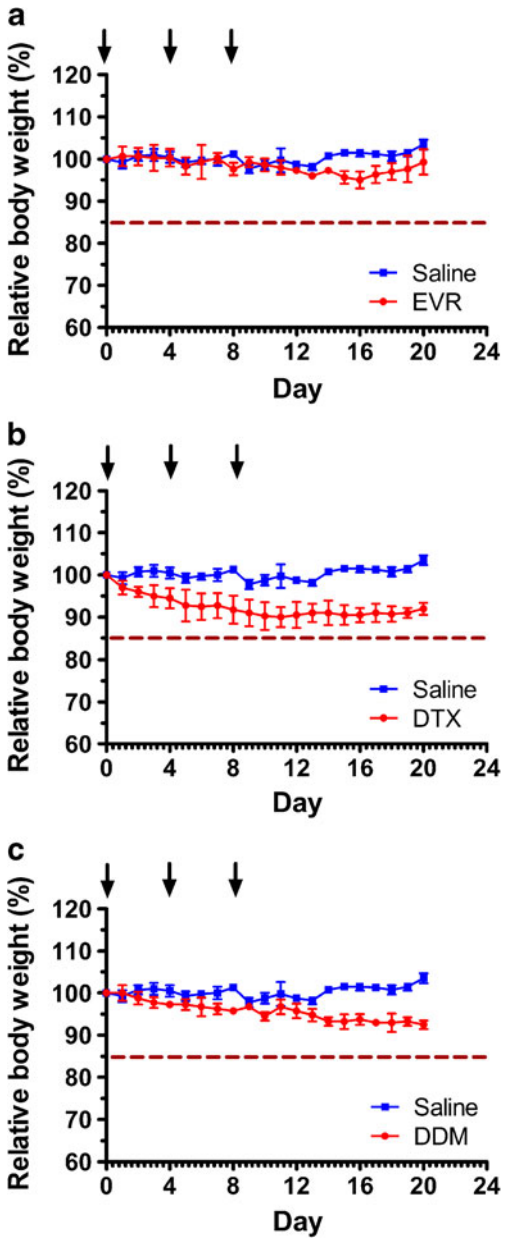

Fig. 10 Relative body weight of mice over time after iv injection of DTX micelle, EVR micelle, or DDM (1:1) on days 0, 4, and 8. (**a**) EVR at 50 mg/kg, (**b**) DTX at 30 mg/kg, (**c**) DTX: EVR (1;1) DDM at 20 mg/kg for each drug total of 40 mg/kg. *Dotted line* represents 15% of the starting average body weight. (Mean ± SD, $n = 4$).

implementation of co-treatment strategies, where multiple mechanisms of drug action can target neovascular angiogenic endothelial cells within the cancer tissue (32). Based on this concept, co-delivery of DTX and EVR, two drugs known to individually inhibit angiogenesis through different pathways, might produce additive/synergistic antiangiogenic effects (14,17,33–35). To achieve this combination, we selected polymeric based nanocarrier as a vehicle for the dual delivery of DTX and EVR. It has been observed that PEG-*b*-PLA micelles can considerably improve the water solubility of DTX as well as other drugs such as rapamycin, 17AAG and etoposide (20,21,25). Therefore, and for the first time, we adapted this platform to formulate the combination of DTX and EVR into DDM along with EVR individual micelles. Two different DTX individual micelles were prepared as previously reported (20,25) PEG_{2000}-*b*-PLA_{1800} DTX individual micelles were more stable than PEG_{4000}-*b*-PLA_{2200} micelle as demonstrated by lower drug precipitation presumably due to better drug-polymer compatibility. PEG_{2000}-*b*-PLA_{1800} individual micelles increased the solubility of DTX to 1.93 mg/mL which is comparable to the published data (25). PEG_{4000}-*b*-PLA_{2200} was used for the formation of EVR individual micelles and DDM due to higher micelles stability at room temperature. We observed similar drug loading for DDM as compared to the individual drug loaded micelles. The ability of the block copolymers to load two drugs into the core of the micelles at same concentrations as individual drugs is a behavior that needs further study, but these findings are consistent with earlier investigators (20,21). EVR micelles and DDM were larger in size≈34 nm in comparison to DTX loaded micelles≈18 nm. This difference in size was observed due to differences in the copolymer block lengths and molecular weights. Other investigators using different block copolymer for the preparation of micelles have reported similar behavior (36). It was reported that block copolymers of high molecular weight result in micelles of higher hydrodynamic radii. According to our findings, PEG_{4000}-*b*-PLA_{2200} always formed micelles of larger diameter irrespective of individual or multiple drug loaded micelles as compared to PEG_{2000}-*b*-PLA_{1800}. Therefore, the block copolymer chosen plays a significant role in determining the size of polymeric micelles formed.

The release of DTX and EVR form the individual and DDM *in vitro* was well fitted with one phase exponential association equation suggesting that the drug(s) release is a diffusion control process and not driven by micelle dissociation process. The release profile of DTX from PEG_{2000}-*b*-PLA_{1800} individual micelles and PEG_{4000}-*b*-PLA_{2200} DDM was almost identical with slight difference in the $t_{1/2}$ value (Fig. 4a). Surprisingly these results clearly showed that different polymer blocks as well as the presence of EVR have minimal effect on DTX release kinetic. On the contrary the release profile of EVR form PEG_{4000}-*b*-PLA_{2000} individual and DDM was influenced by the presence of DTX (Fig. 4b). DDM released 49.2±0.9% of total amount of EVR in 48 h with $r^2 = 0.955$. In contrast faster release was seen for EVR from PEG_{4000}-*b*-PLA_{2000} individual micelle with about 50% of the EVR released occurring in 35 h. Additionally more EVR was released from the individual micelles at 60.0±2.4% in 48 h. The difference in the release profile between EVR micelles can be contributed to the burst effect in drug release exhibited by the EVR individual micelles, in which about 20% of the drug was released within the first 30 min of the release experiment (Fig. 4b). The burst effect also affected the data goodness of fit as reflected by an r^2 value of 0.820. On the

other hand EVR release from DDM exhibited a weaker burst effect with less than 10% of the drug being released within the first 30 min and with a goodness of fit r^2 value of 0.955.

This discrepancy in the release profile of the EVR from both micelles can be clearly contributed to the presence of DTX. It can be speculated that the presence DTX in the DDM enhanced the compatibility between the EVR and the polymer and thereby EVR release profile in the DDM resulted in a smaller burst effect. A similar profile has been seen in other multiple-drug loaded polymeric micelles, Shen *et al*. showed that paclitaxel release profile was significantly different between individual micelles and multiple-drug loaded micelles (22). In the same study paclitaxel release from individual micelle could not be collected as the drug precipitated from the micelles during the study. On the other hand, when paclitaxel was co-loaded with 17AAG the paclitaxel was retained in the micelle during the release study and the $t_{1/2}$ of the paclitaxel was 5.01 h. Additionally, when paclitaxel was loaded with 17AAG and rapamycin the release profile of paclitaxel was different from paclitaxel/17AAG micelle with $t_{1/2}=9.20$ h (22). Shen *et al*. hypothesize that the difference in micelle stability and drug release profile between individual drug loaded micelles and multiple drug loaded micelles is due to possible intermolecular interaction among drugs in the core region of micelle (22).

DTX and EVR individual micelles exhibited dose dependent antiproliferative response on HUVEC cells (Fig. 6). The IC_{50} values for the individual micelles were slightly higher than the published data for the free drug which are 0.5 nM for DTX and 0.12 nM for EVR (13,16). The difference in IC_{50} values between the free drug and drug individual micelle is possibly due to the high stability of the micelles *in vitro* which results in lower free drug being available to exert its effect on the cells. The combination of the DTX and EVR (1:1) molar ratio in DDM exhibited strong synergistic inhibition on HUVEC proliferation over wide range of doses (Figs. 6 and 7).

Endothelial tube formation involves multiple steps such as attachment, proliferation and migration prior to tube formation process. Tube formation is initiated with attachment of endothelial cells on the basement matrix and then is followed by migration of these cells towards each other to eventually form tubes (37). Our data has shown this process can be inhibited at various concentrations of DTX and EVR individual and DDM (Fig. 8). In the tube formation experiment, DTX at 1 nM showed significant reduction in the tube formation area compared to control, the result is in agreement with earlier findings were taxanes exert antiangiogenic effects at lower concentrations than their IC_{50} (11–13). EVR individual micelle significantly reduced the tube formation area at 1,000 nM a higher concentration than its IC_{50}. The discrepancy in potency of EVR individual micelles in HUVEC proliferation and tube formation might be contributed to the micelle stability and to the short time frame for the tube formation experiment. Interestingly the treatment of the HUVEC with a combination of DTX and EVR micelles at 0.5 and 500 nM respectively inhibited the tube formation significantly compared to DTX micelle alone at 1 nM, the data clearly shows that EVR can intensify the DTX inhibitory effect in HUVEC tube formation.

Real time migration assay with the DDM DTX:EVR, each at 0.005 nM (total of 0.01 nM), demonstrated synergistic/additive inhibition in HUVEC cell migration (Fig. 9). It was observed that DTX individual PEG_{2000}-*b*-PLA_{1800} micelles at 0.005 nM concentrations inhibited HUVEC migration. Meanwhile EVR loaded PEG_{4000}-*b*-PLA_{2200} micelles at 0.005 nM did not inhibit HUVEC migration; however EVR micelles at concentrations above 0.005 nM inhibited cell migration. We observed that EVR enhanced the antimigratory activity of DTX at 0.005 nM a concentration at which individual DTX micelles has weaker inhibition on endothelial cell migration. These results suggest that the combined treatment of DTX and EVR inhibits HUVEC cell migration by synergistic/additive response. Cell migration process is regulated through reorientation of centrosome in the intended direction of movement (38). It was also observed that change in microtubule plasticity can alter the reorientation of the centrosome (38). Based on this mechanism, in our study we postulate that EVR potentiates the antimigratory effect of DTX on endothelial cells (Fig. 9) by changing the microtubule plasticity. Further studies are required to delineate the exact molecular mechanism behind the enhanced migratory activity in the case of DDM. Our study provides strong evidence that combined treatment of DTX and EVR DDM is advantageous in comparison to individual drugs for antiangiogenic treatment due to its inhibition of three major cascade events in the angiogenic process.

The acute toxicity of the individual and DDM was examined in mice. The MTD for EVR individual micelles was 50 mg/kg which much higher than any published data, for example Iwase, *et.al* showed the MTD of liposomal EVR formulation in mice treated by intravenous injection was 5 mg/kg (24). The MTD for DTX micelles in our work was higher than Taxotere® at 20 mg/kg for similar dosing regimen (39). The DDM showed MTD at 20 mg/kg (for each drug, total of 40 mg/kg). For all micelles the MTD values were much higher than the required concentration to produce the anticancer or the antiangiogenic *in vivo* models as well as for clinical setting (40). In conclusion, we were able to formulate new micellar nanocarriers for EVR alone or in combination with DTX as a DDM. Also were able to show for the first time that the combination of DTX and EVR in DDM inhibited angiogenesis by affecting different cascade events in angiogenesis process with more potency than individual DTX or EVR micelles. Finally all micellar nanocarriers showed no acute toxicity at clinically relevant concentrations in mice.

ACKNOWLEDGMENTS AND DISCLOSURES

This study was supported by the grant from AACP New Pharmacy Faculty Research Award Program, Medical Research Foundation of Oregon New Investigator Grant and Oregon State University-Startup fund.

REFERENCES

1. Longo R, Sarmiento R, Fanelli M, Capaccetti B, Gattuso D, Gasparini G. Anti-angiogenic therapy: rationale, challenges and clinical studies. Angiogenesis. 2002;5(4):237–56.
2. Carmeliet P. Angiogenesis in health and disease. Nat Med. 2003;9(6):653–60.
3. Folkman J. Endogenous angiogenesis inhibitors. APMIS. 2004;112(7–8):496–507.
4. Li W, Hutnik M, Smith R, Li V. Understanding angiogenesis http://www.angio.org/ua.php (accessed April 16 2013).
5. Folkman J. Angiogenesis. Annu Rev Med. 2006;57:1–18.
6. Bocci Gand Loupakis F. The possible role of chemotherapy in antiangiogenic drug resistance. Med Hypotheses. 2012;78(5):646–8.
7. Guba M, von Breitenbuch P, Steinbauer M, Koehl G, Flegel S, Hornung M, *et al*. Rapamycin inhibits primary and metastatic tumor growth by antiangiogenesis: involvement of vascular endothelial growth factor. Nat Med. 2002;8(2):128–35.
8. Miller KD, Sweeney CJ, Sledge Jr GW. Redefining the target: chemotherapeutics as antiangiogenics. J Clin Oncol. 2001;19(4):1195–206.
9. Bocci G, Francia G, Man S, Lawler J, Kerbel RS. Thrombospondin 1, a mediator of the antiangiogenic effects of low-dose metronomic chemotherapy. Proc Natl Acad Sci U S A. 2003;100(22):12917–22.
10. Bocci G, Nicolaou KC, Kerbel RS. Protracted low-dose effects on human endothelial cell proliferation and survival in vitro reveal a selective antiangiogenic window for various chemotherapeutic drugs. Cancer Res. 2002;62(23):6938–43.
11. Hayot C, Farinelle S, De Decker R, Decaestecker C, Darro F, Kiss R, *et al*. In vitro pharmacological characterizations of the anti-angiogenic and anti-tumor cell migration properties mediated by microtubule-affecting drugs, with special emphasis on the organization of the actin cytoskeleton. Int J Oncol. 2002;21(2):417–25.
12. Wang J, Lou P, Lesniewski R, Henkin J. Paclitaxel at ultra low concentrations inhibits angiogenesis without affecting cellular microtubule assembly. Anticancer Drugs. 2003;14(1):13–9.
13. Vacca A, Ribatti D, Iurlaro M, Merchionne F, Nico B, Ria R, *et al*. Docetaxel versus paclitaxel for antiangiogenesis. J Hematother Stem Cell Res. 2002;11(1):103–18.
14. Murtagh J, Lu H, Schwartz EL. Taxotere-induced inhibition of human endothelial cell migration is a result of heat shock protein 90 degradation. Cancer Res. 2006;66(16):8192–9.
15. Manegold PC, Paringer C, Kulka U, Krimmel K, Eichhorn ME, Wilkowski R, *et al*. Antiangiogenic therapy with mammalian target of rapamycin inhibitor RAD001 (Everolimus) increases radiosensitivity in solid cancer. Clin Cancer Res. 2008;14(3):892–900.
16. Lane HA, Wood JM, McSheehy PM, Allegrini PR, Boulay A, Brueggen J, *et al*. mTOR inhibitor RAD001 (everolimus) has antiangiogenic/vascular properties distinct from a VEGFR tyrosine kinase inhibitor. Clin Cancer Res. 2009;15(5):1612–22.
17. Faivre S, Kroemer G, Raymond E. Current development of mTOR inhibitors as anticancer agents. Nat Rev Drug Discov. 2006;5(8):671–88.
18. Adams ML, Lavasanifar A, Kwon GS. Amphiphilic block copolymers for drug delivery. J Pharm Sci. 2003;92(7):1343–55.
19. Oerlemans C, Bult W, Bos M, Storm G, Nijsen JF, Hennink WE. Polymeric micelles in anticancer therapy: targeting, imaging and triggered release. Pharm Res. 2010;27(12):2569–89.
20. Shin HC, Alani AW, Rao DA, Rockich NC, Kwon GS. Multi-drug loaded polymeric micelles for simultaneous delivery of poorly soluble anticancer drugs. J Control Release. 2009;140(3):294–300.
21. Shin HC, Alani AW, Cho H, Bae Y, Kolesar JM, Kwon GS. A 3-in-1 polymeric micelle nanocontainer for poorly water-soluble drugs. Mol Pharm. 2011;8(4):1257–65.
22. Hasenstein JR, Shin HC, Kasmerchak K, Buehler D, Kwon GS, Kozak KR. Antitumor activity of Triolimus: a novel multidrug-loaded micelle containing Paclitaxel, Rapamycin, and 17-AAG. Mol Cancer Ther. 2012;11(10):2233–42.
23. Mazzaferro S, Bouchemal K, Gallard JF, Iorga BI, Cheron M, Gueutin C, *et al*. Bivalent sequential binding of docetaxel to methyl-beta-cyclodextrin. Int J Pharm. 2011;416(1):171–80.
24. Iwase Yand Maitani Y. Preparation and in vivo evaluation of liposomal everolimus for lung carcinoma and thyroid carcinoma. Biol Pharm Bull. 2012;35(6):975–9.
25. Lee SW, Yun MH, Jeong SW, In CH, Kim JY, Seo MH, *et al*. Development of docetaxel-loaded intravenous formulation, Nanoxel-PM using polymer-based delivery system. J Control Release. 2011;155(2):262–71.
26. Maciag T, Kadish J, Wilkins L, Stemerman MB, Weinstein R. Organizational behavior of human umbilical vein endothelial cells. J Cell Biol. 1982;94(3):511–20.
27. Vailhe B, Vittet D, Feige JJ. In vitro models of vasculogenesis and angiogenesis. Lab Investig. 2001;81(4):439–52.
28. Kim SC, Kim DW, Shim YH, Bang JS, Oh HS, Wan Kim S, *et al*. In vivo evaluation of polymeric micellar paclitaxel formulation: toxicity and efficacy. J Control Release. 2001;72(1–3):191–202.
29. Chou T-C, Martin N. CompuSyn, CompuSyn software for drug combinations and for general dose-effect analysis, and user's guide. Paramus: ComboSyn, Inc.; 2007.
30. Chou TC, Talalay P. Quantitative analysis of dose-effect relationships: the combined effects of multiple drugs or enzyme inhibitors. Adv Enzym Regul. 1984;22:27–55.
31. Schneider CA, Rasband WS, Eliceiri KW. NIH Image to ImageJ: 25 years of image analysis. Nat Methods. 2012;9(7):671–5.
32. Pasquier E, Andre N, Braguer D. Targeting microtubules to inhibit angiogenesis and disrupt tumour vasculature: implications for cancer treatment. Curr Cancer Drug Targets. 2007;7(6):566–81.
33. Pazdur R. FDA approval for doctaxel. http://www.cancer.gov/cancertopics/druginfo/fda-docetaxel (accessed April 21 2013).
34. Benjamin D, Colombi M, Moroni C, Hall MN. Rapamycin passes the torch: a new generation of mTOR inhibitors. Nat Rev Drug Discov. 2011;10(11):868–80.
35. Pazdur R. FDA Approval for Everolimus. http://www.cancer.gov/cancertopics/druginfo/fda-everolimus#Anchor-Breast (accessed April 21 2013).
36. Huh KM, Lee SC, Cho YW, Lee J, Jeong JH, Park K. Hydrotropic polymer micelle system for delivery of paclitaxel. J Control Release. 2005;101(1–3):59–68.
37. Papetti M, Herman IM. Mechanisms of normal and tumor-derived angiogenesis. Am J Physiol Cell Physiol. 2002;282(5):C947–70.
38. Hotchkiss KA, Ashton AW, Mahmood R, Russell RG, Sparano JA, Schwartz EL. Inhibition of endothelial cell function in vitro and angiogenesis in vivo by docetaxel (Taxotere): association with impaired repositioning of the microtubule organizing center. Mol Cancer Ther. 2002;1(13):1191–200.
39. Bradshaw-Pierce EL, Eckhardt SG, Gustafson DL. A physiologically based pharmacokinetic model of docetaxel disposition: from mouse to man. Clin Cancer Res. 2007;13(9):2768–76.
40. Grant DS, Williams TL, Zahaczewsky M, Dicker AP. Comparison of antiangiogenic activities using paclitaxel (taxol) and docetaxel (taxotere). Int J Cancer. 2003;104(1):121–9.